Biogeosciences

Open Access

Supplement of

Revisiting the applicability and constraints of molybdenum- and uranium-based paleo redox proxies: comparing two contrasting sill fjords

K. Mareike Paul et al.

Correspondence to: K. Mareike Paul (mareike.paul@helsinki.fi)

Table of contents

Koljö Fjord

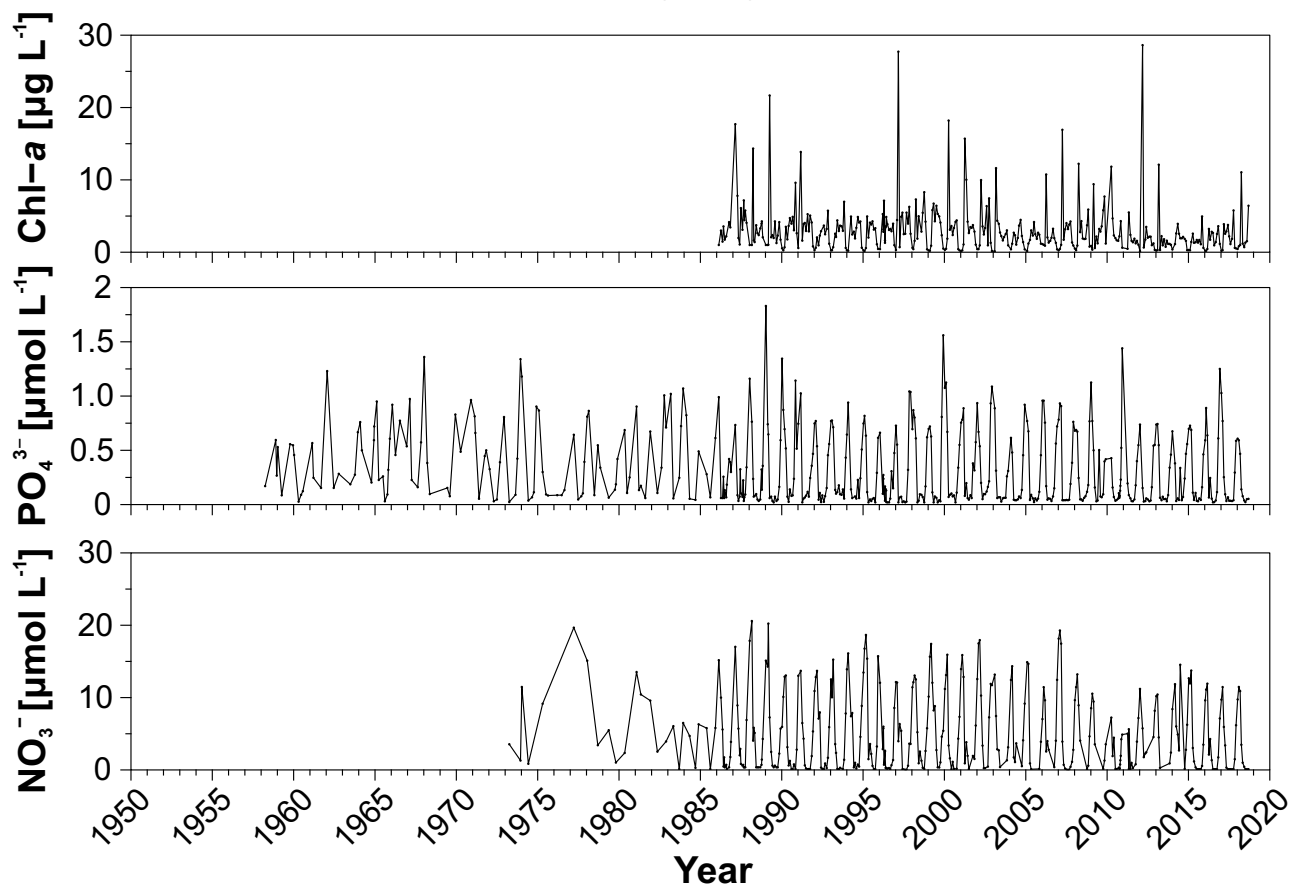**Figure S1.** Bottom water nutrient (PO_4^{3-}+NO_3^-) and chlorophyll-*a* (average 0−10 m) monitoring data for Koljö Fjord between 1950 and 2018 (SMHI, 2022).

Table S1a. List of blanks (1 and 2) for Gullmar Fjord, which were used to correct the sequential extraction data of U, Mo, Fe, Mn, Al, Ca, and S in fractions F1–F6. Blanks were treated the same as the samples in the sequential extraction procedure. The average (highlighted in italic) of the two blanks were subtracted from each sample of each fraction. In case where blanks exceeded the measured element in sample, the analyzed value was returned as 0 – corresponding blanks are highlighted in **bold**. Sulfur contents in F3 and F5 could not be determined (n.d). In F6, except for S blanks were generally below detection limits; for blank correction threshold values were used.

	F1	F2	F3	F4	F5	F6
Gullmar Fjord						
Uranium [ppb]						
Blank 1	0.016	0.019	0.004	-0.005	-0.003	<0.001
Blank 2	0.016	0.021	0.010	0.008	-0.003	<0.001
Average Blank	*0.016*	*0.020*	*0.007*	*0.002*	*-0.003*	*0.001*
Molybdenum [ppb]						
Blank 1	0.477	**17.821**	5.386	0.118	-0.017	<0.200
Blank 2	0.430	**16.999**	5.663	0.144	-0.029	<0.200
Average Blank	*0.454*	***17.410***	*5.524*	*0.131*	*-0.023*	*0.200*
Iron [ppm]						
Blank 1	0.006	0.011	0.149	0.082	0.007	<20.000
Blank 2	0.063	0.041	0.185	0.169	0.005	<20.000
Average Blank	*0.035*	*0.026*	*0.167*	*0.125*	*0.006*	*20.000*
Manganese [ppm]						
Blank 1	0.045	0.008	0.012	0.002	0.001	<1.900
Blank 2	0.058	0.028	0.030	0.006	0.000	<1.900
Average Blank	*0.051*	*0.018*	*0.021*	*0.004*	*0.001*	*1.900*
Aluminum [ppm]						
Blank 1	0.0005	0.016	0.018	0.167	0.824	<30.900
Blank 2	-0.0006	0.182	0.017	0.348	0.202	<30.900
Average Blank	*-0.0000*	*0.099*	*0.018*	*0.257*	*0.513*	*30.900*
Calcium [ppm]						
Blank 1	8.664	1.716	0.265	0.238	0.196	<53.000
Blank 2	8.792	1.885	0.226	0.280	0.152	<53.000
Average Blank	*8.728*	*1.801*	*0.246*	*0.259*	*0.174*	*53.000*
Sulfur [ppm]						
Blank 1	159.726	26.055	n.d.	0.238	n.d.	16.467
Blank 2	169.496	24.797	n.d.	0.280	n.d.	7.303
Average Blank	*164.611*	*25.426*	*n.d.*	*0.259*	*n.d.*	*11.885*

Table S1b. List of blanks (3 and 4) for Koljö Fjord. For analytical and procedural details, see Table S1. Sulfur contents in F3 could not be determined (n.d). In F6, except for S blanks were generally below detection limits; for blank correction threshold value were used.

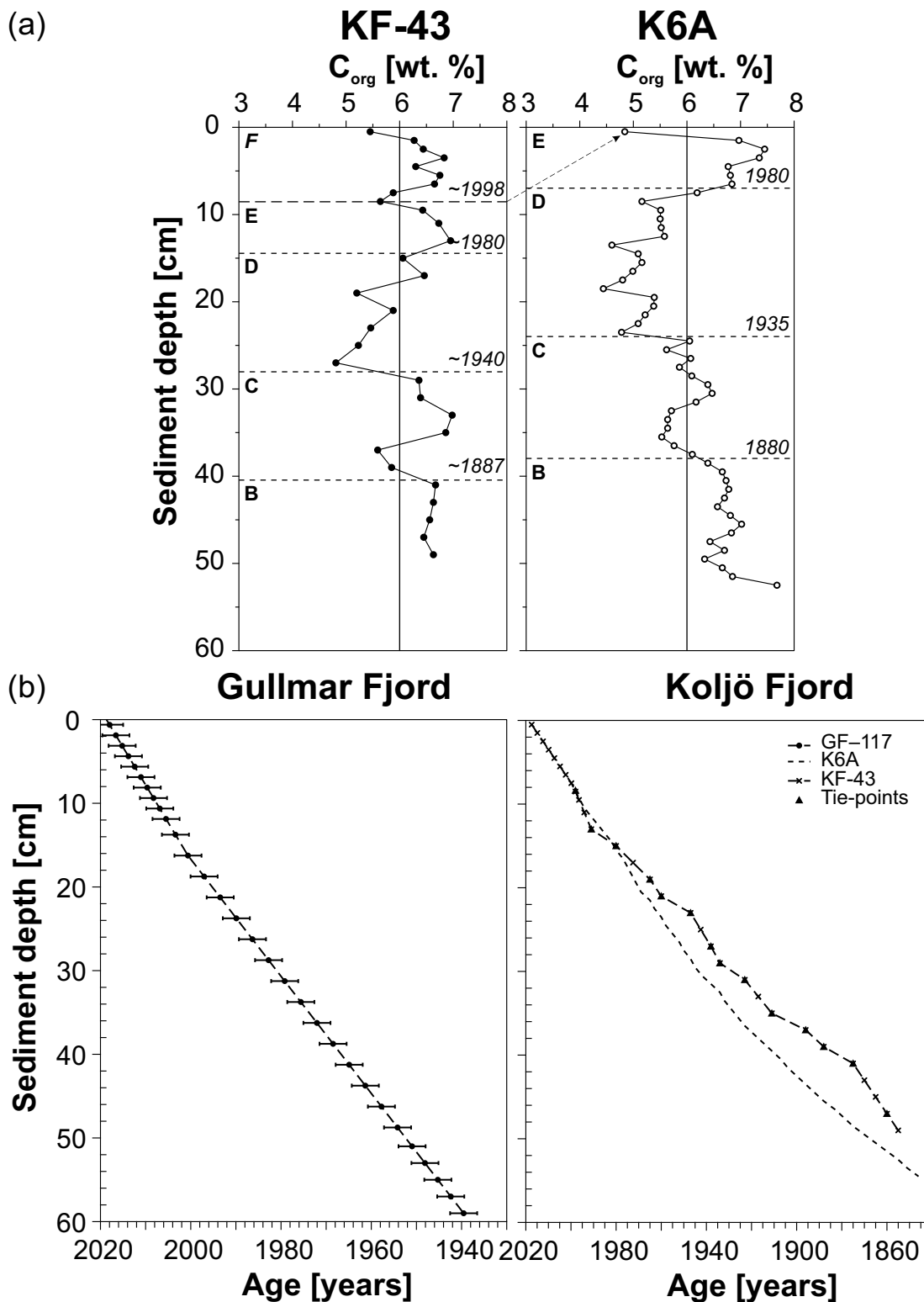|	F1	F2	F3	F4	F5	F6
Koljö Fjord						
Uranium [ppb]						
Blank 3	0.009	0.061	0.072	0.017	0.006	<0.001
Blank 4	0.007	0.037	0.031	-0.005	0.001	<0.001
Average Blank	*0.008*	*0.049*	*0.052*	*0.006*	*0.003*	*0.001*
Molybdenum [ppb]						
Blank 3	0.854	**41.626**	5.776	0.089	0.003	<0.200
Blank 4	0.733	**42.403**	6.349	0.103	-0.019	<0.200
Average Blank	*0.793*	***42.015***	*6.063*	*0.096*	*-0.008*	*0.200*
Iron [ppm]						
Blank 3	0.012	0.006	0.176	0.036	0.004	<20.000
Blank 4	0.025	0.015	0.154	0.052	0.004	<20.000
Average Blank	*0.018*	*0.010*	*0.165*	*0.044*	*0.004*	*20.000*
Manganese [ppm]						
Blank 3	0.039	0.038	0.018	0.006	0.0002	<1.900
Blank 4	-0.001	0.006	0.020	0.007	0.0002	<1.900
Average Blank	*0.019*	*0.022*	*0.019*	*0.007*	*0.0002*	*1.900*
Aluminum [ppm]						
Blank 3	-0.011	0.003	0.026	0.019	0.005	<30.900
Blank 4	-0.003	0.005	0.085	0.033	0.003	<30.900
Average Blank	*-0.007*	*0.004*	*0.056*	*0.026*	*0.004*	*30.900*
Calcium [ppm]						
Blank 3	8.912	8.287	0.963	0.474	0.535	<53.000
Blank 4	2.168	2.211	0.817	0.486	0.463	<53.000
Average Blank	*5.540*	*5.249*	*0.890*	*0.480*	*0.499*	*53.000*
Sulfur [ppm]						
Blank 3	173.900	**179.026**	n.d.	162.769	0.702	7.541
Blank 4	122.955	**142.675**	n.d.	97.866	0.557	12.508
Average Blank	*148.427*	***160.850***	*n.d.*	*130.318*	*0.630*	*10.025*

Figure S2. (a) C_{org} based age model of KF-43 (left panel) based on a previously dated sediment core K6A (right panel, Filipsson and Nordberg, 2004a) from the same sampling location at Koljö Fjord. The letters B-E refer to the units described in Filipsson and Nordberg (2004a) based on the C_{org} content (6 wt. % threshold). Based on this approach, we added the unit *F*, which covers the period from 1998 (end of unit E, see dashed arrow) to 2018. (b) Left panel: age model for Gullmar Fjord (GF-117) based on average sedimentation rates estimated by ^{210}Pb dating and biostratigraphy (Nordberg et al., 2000; Filipsson and Nordberg, 2004b). Error bars, representing a margin of error of ±3 years for the ^{210}Pb ages, were added to the calculated ages (as per Roos, 1989 and Nordberg et al., 2000). Right panel: age model for Koljö Fjord (KF-43) based on tuning with the dated C_{org} (a) using QAnalySeries (Kotov and Paelike, 2018). The black triangles represent the 14 tie-points used for the tuning. The dashed line shows the original depth vs. age model for K6A, displaced by 8.5 cm downwards to account for sediment accumulation between 1998 (sampling year of K6A) –2018 (sampling year of KF-43, see text).
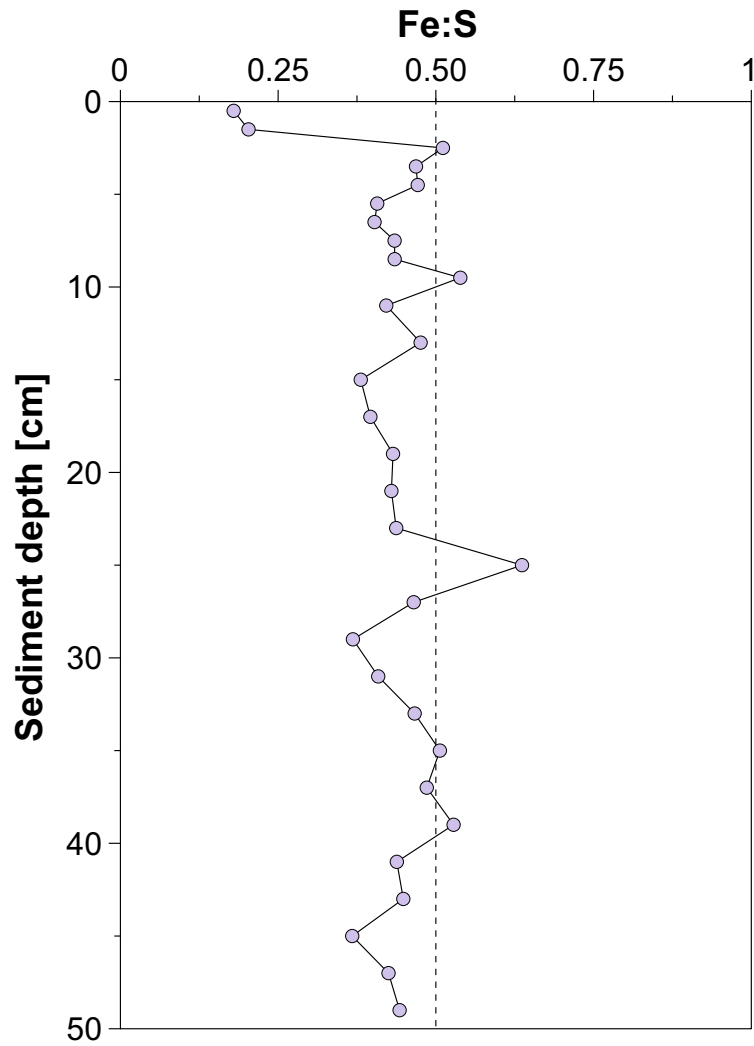
Koljö Fjord

Fe:S

Figure S3. Fe:S ratio at Koljö Fjord based on Fe and S contents in fraction F5 from the extraction protocol (Table 1 main text). The dashed line shows the 1:2 ratio, which is indicative for pyrite (FeS_2).
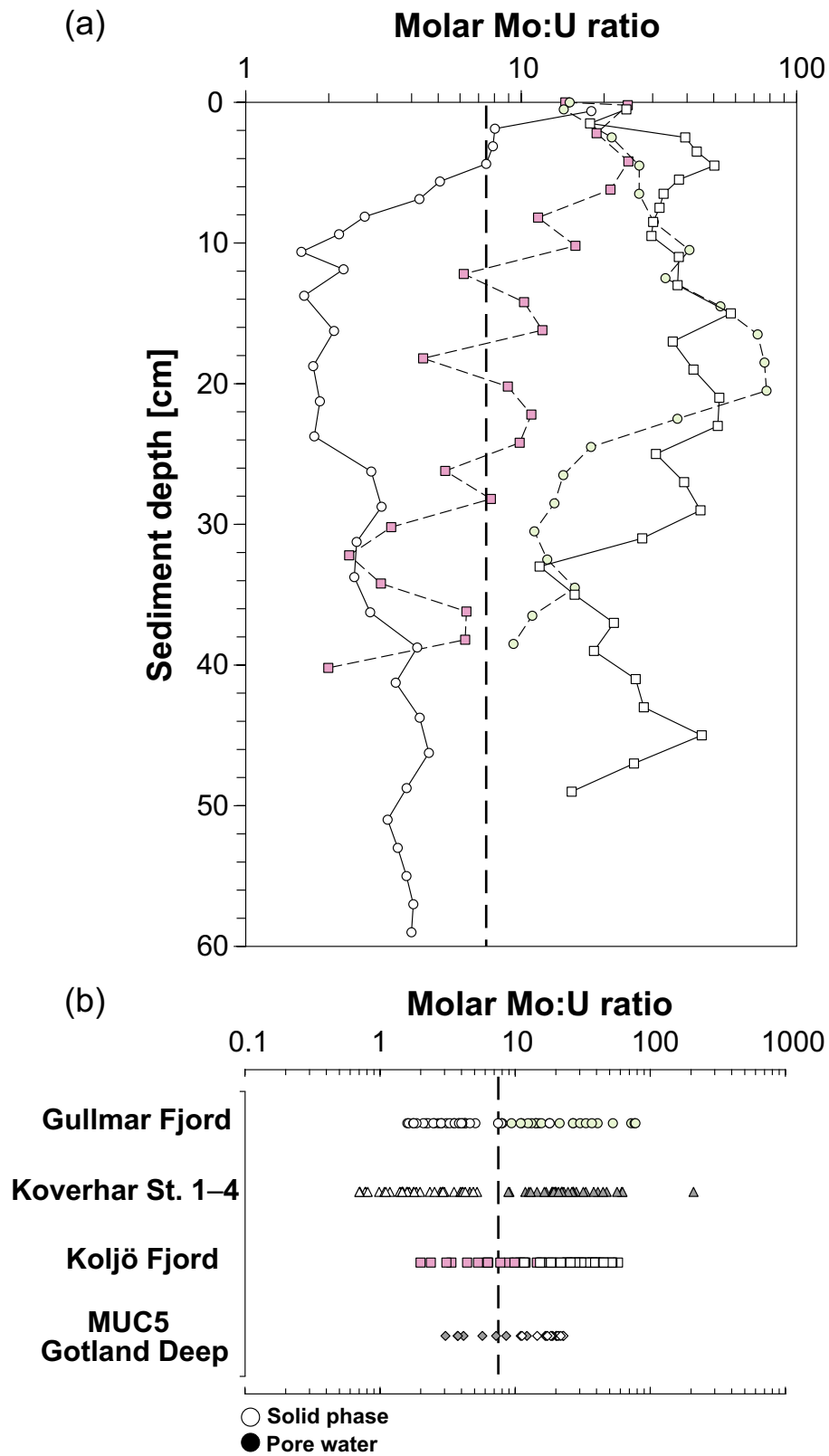
Figure S4. (a) Pore water (filled symbols) and solid-phase (empty symbols) molar Mo:U ratio at Gullmar– and Koljö Fjord, (b) compared to literature data (Koverhar St. 1–4 was taken from Jokinen et al., 2020, and MUC5 from Scholz et al., 2013). In both panels, the Mo:U ratio is shown on a $\log_{10}$ scale.
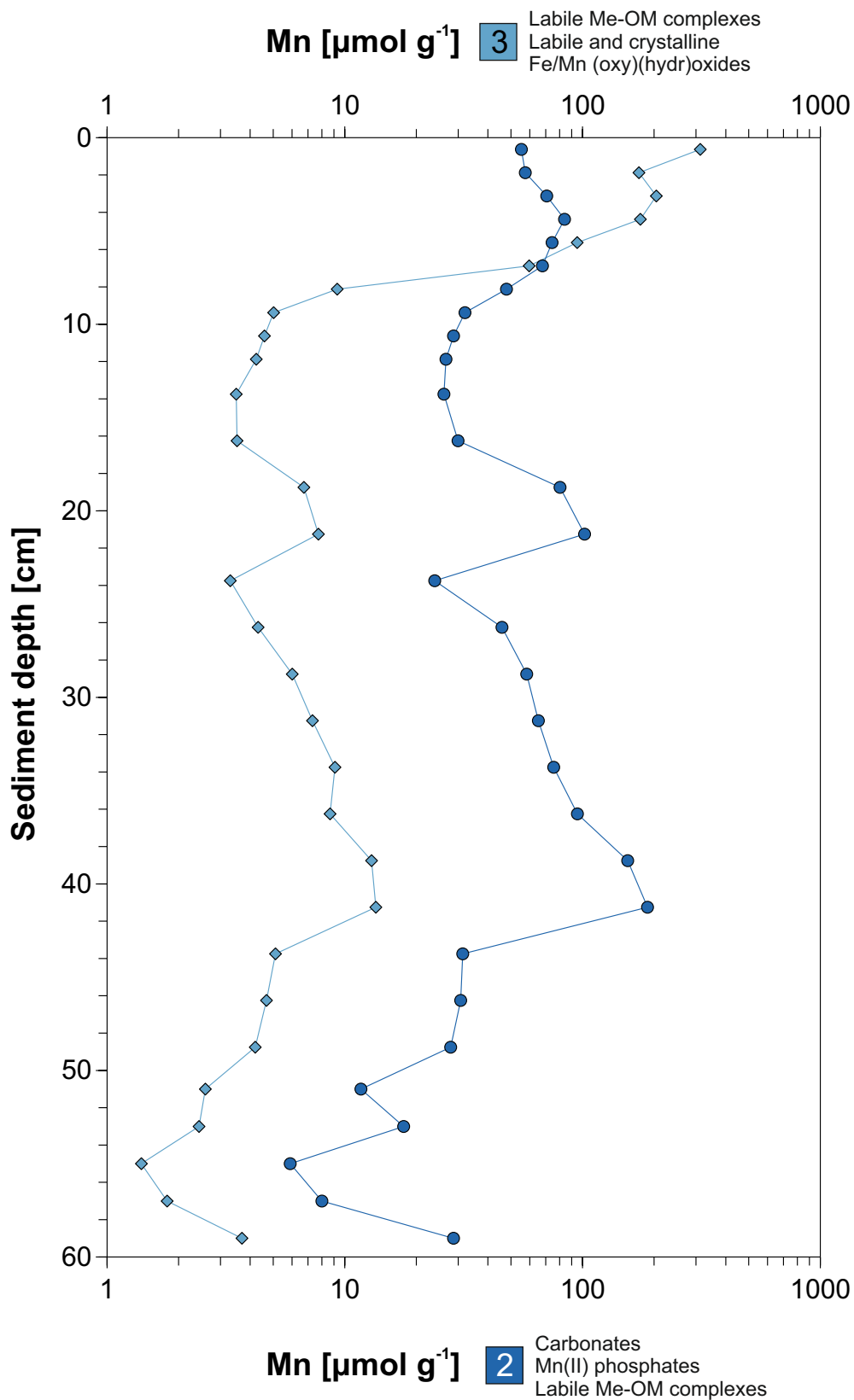
Figure S5. Sediment covariation between Mn in F2 (dark blue circles, lower x-axis) and F3 (middle blue diamonds, upper x-axis) at Gullmar Fjord. Note that Mn contents are given on a $\log_{10}$ scale.
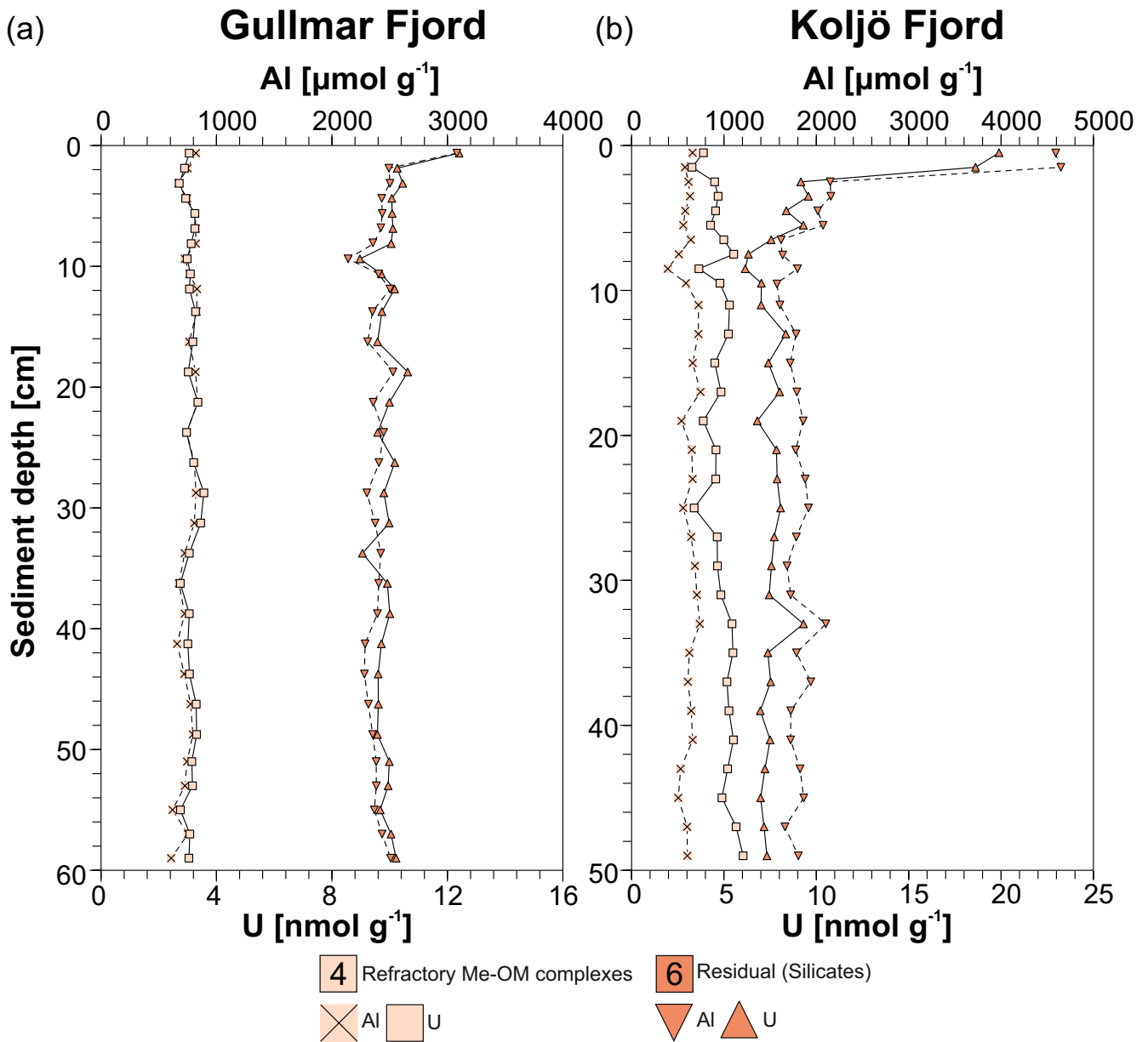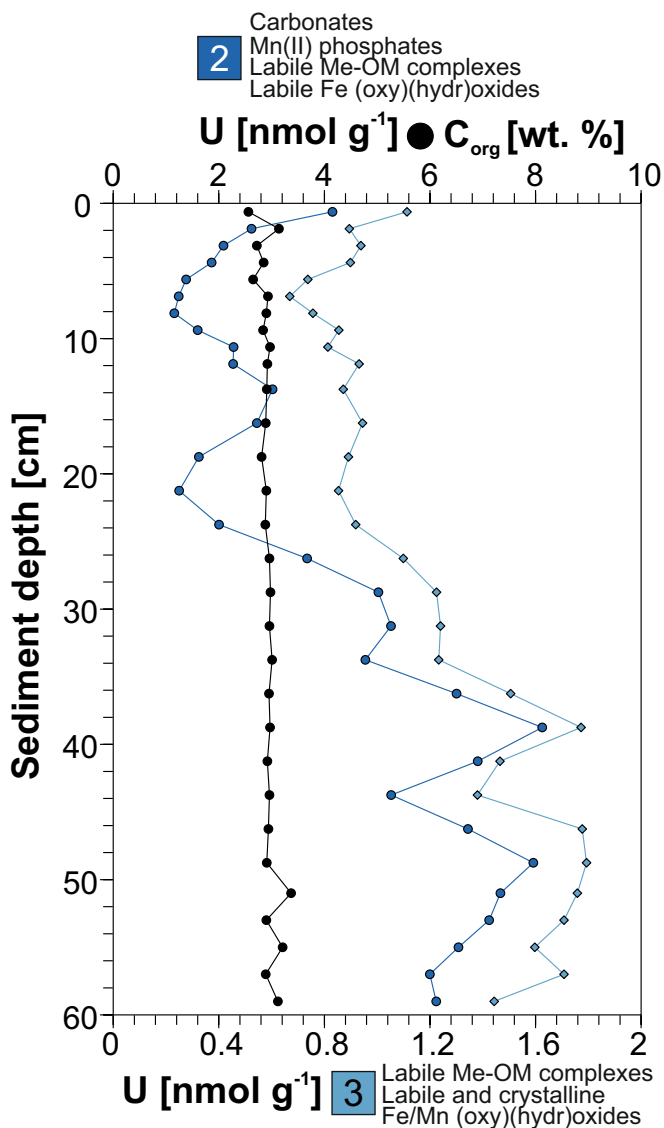
Figure S6. Sediment covariation between (a) U and Al in F4 and F6 at Gullmar– and (b) Koljö Fjord. Light orange filled squares represent U in F4, and light orange filled squares with a black cross show Al in F4. Orange filled triangles represent U in F6, inversed orange filled triangles show Al in F6.
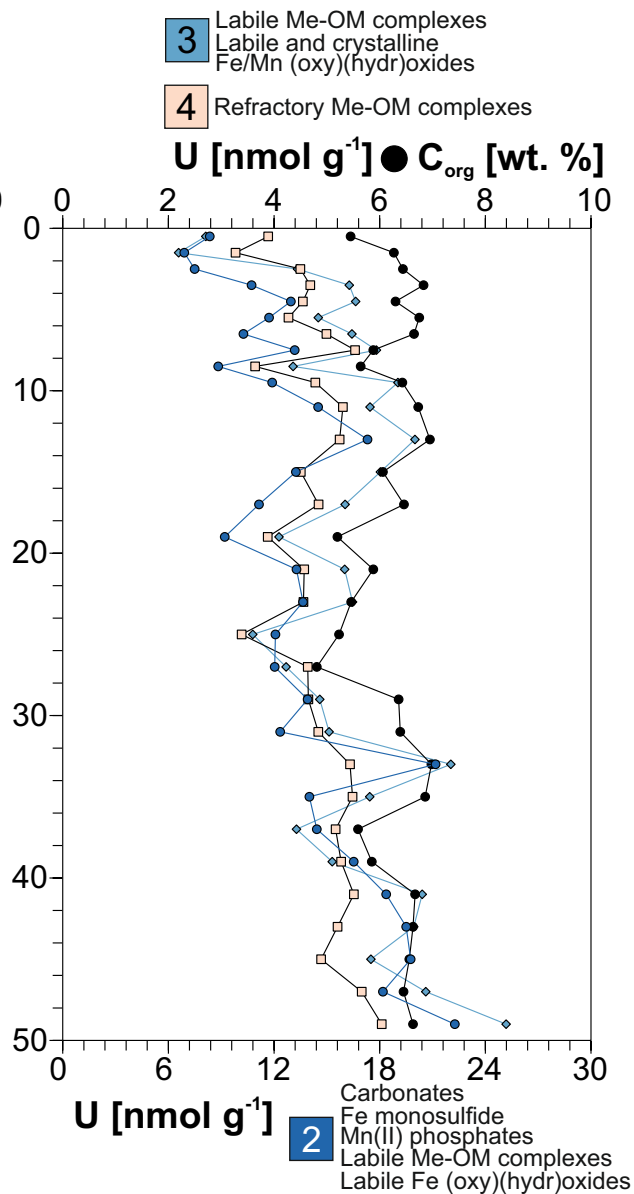
Figure S7. Sediment covariation between (a) C$_{org}$ (black circles) and U in F2 (dark blue circles), F3 (middle blue diamonds), and F4 (light orange squares) at Gullmar – and (b) Koljö Fjord.
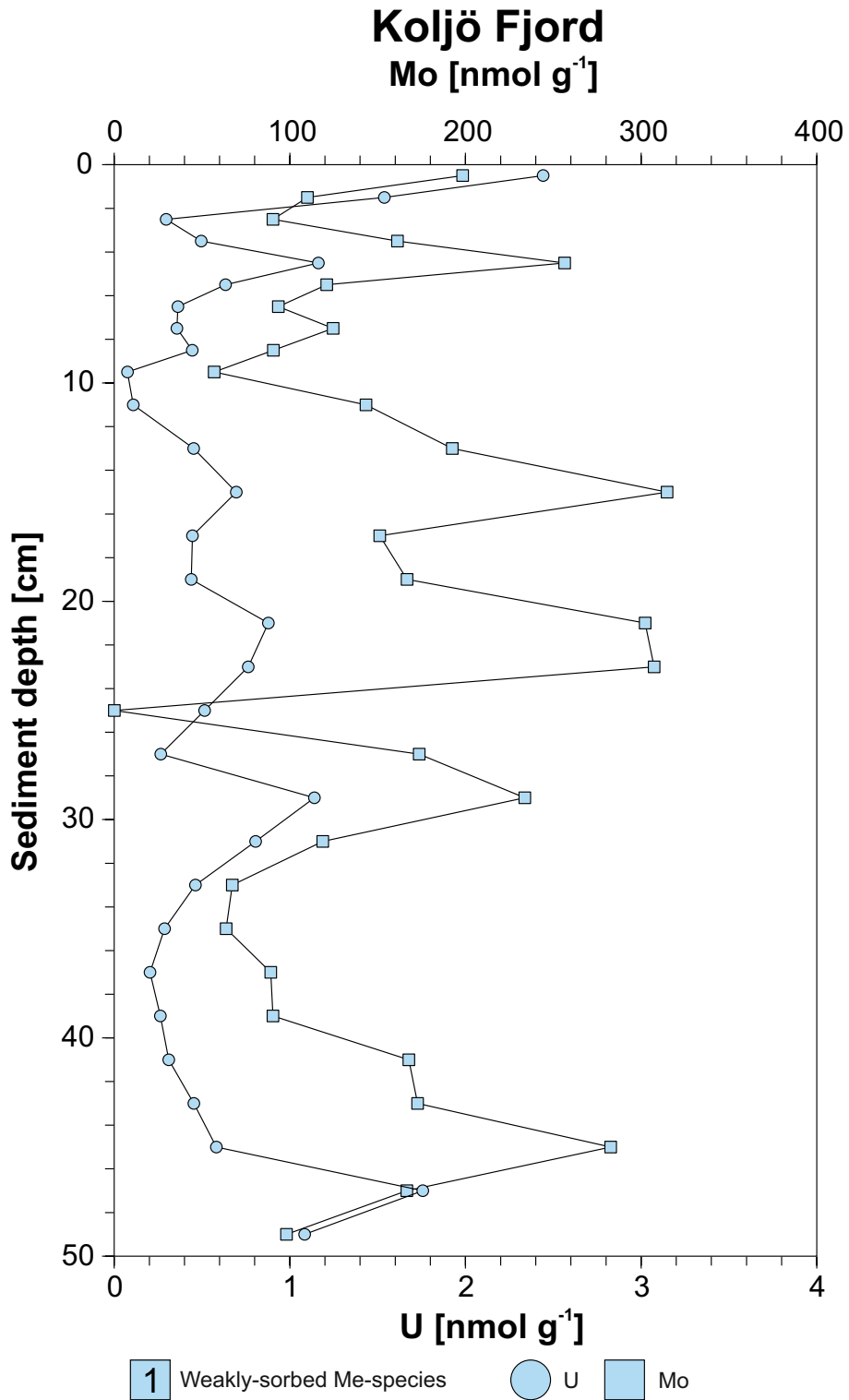
Figure S8. Sediment covariation between Mo (light blue squares, upper x-axis) and U (light blue circles, lower x-axis) in F1 at Koljö Fjord.
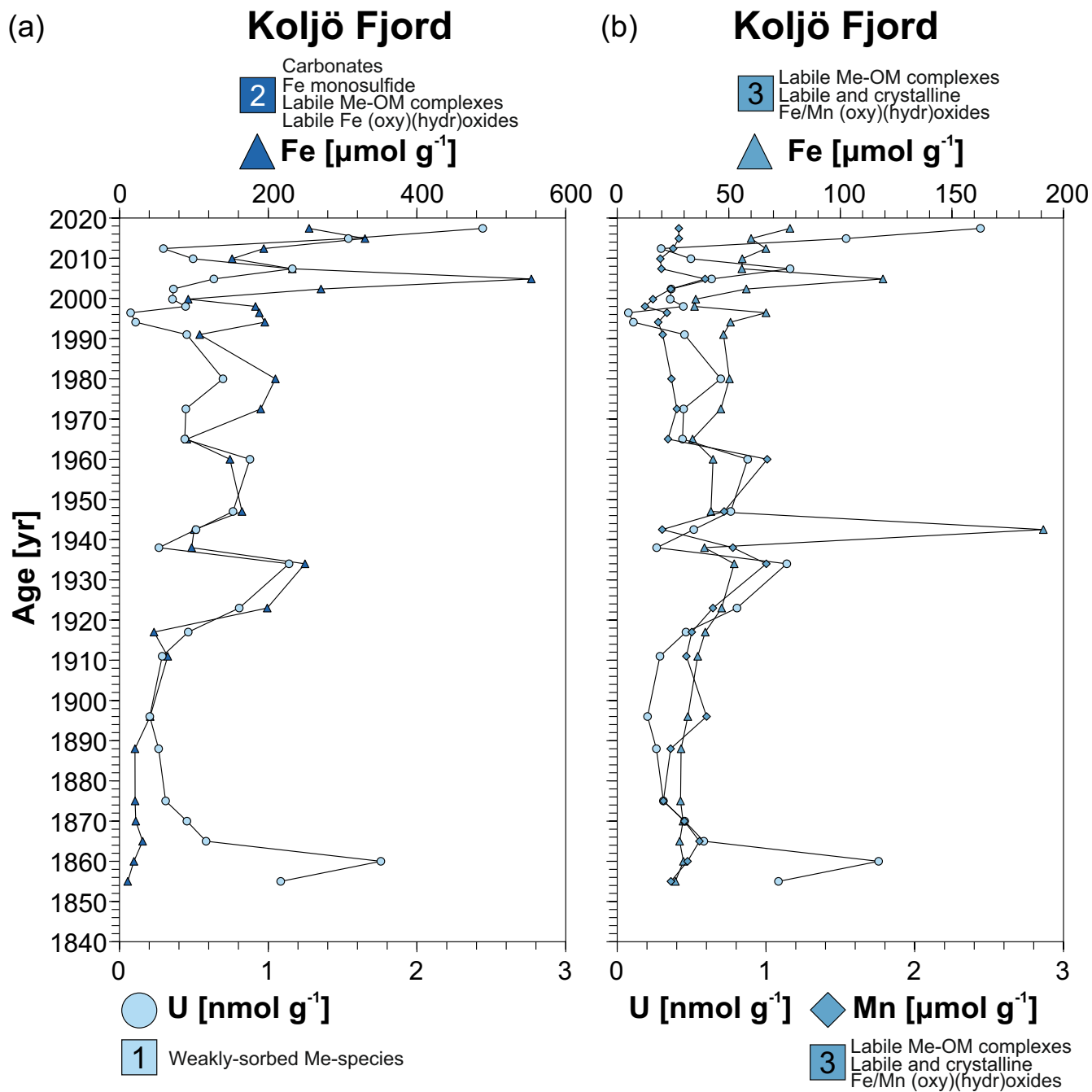
Figure S9. Covariation between (a) U in F1 (light blue circles, lower x-axis) with Fe in F2 (dark blue triangles), and (b) between U in F1 (light blue circles) with Mn (middle blue diamonds) and Fe (middle blue triangles) in F3 at Koljö Fjord.
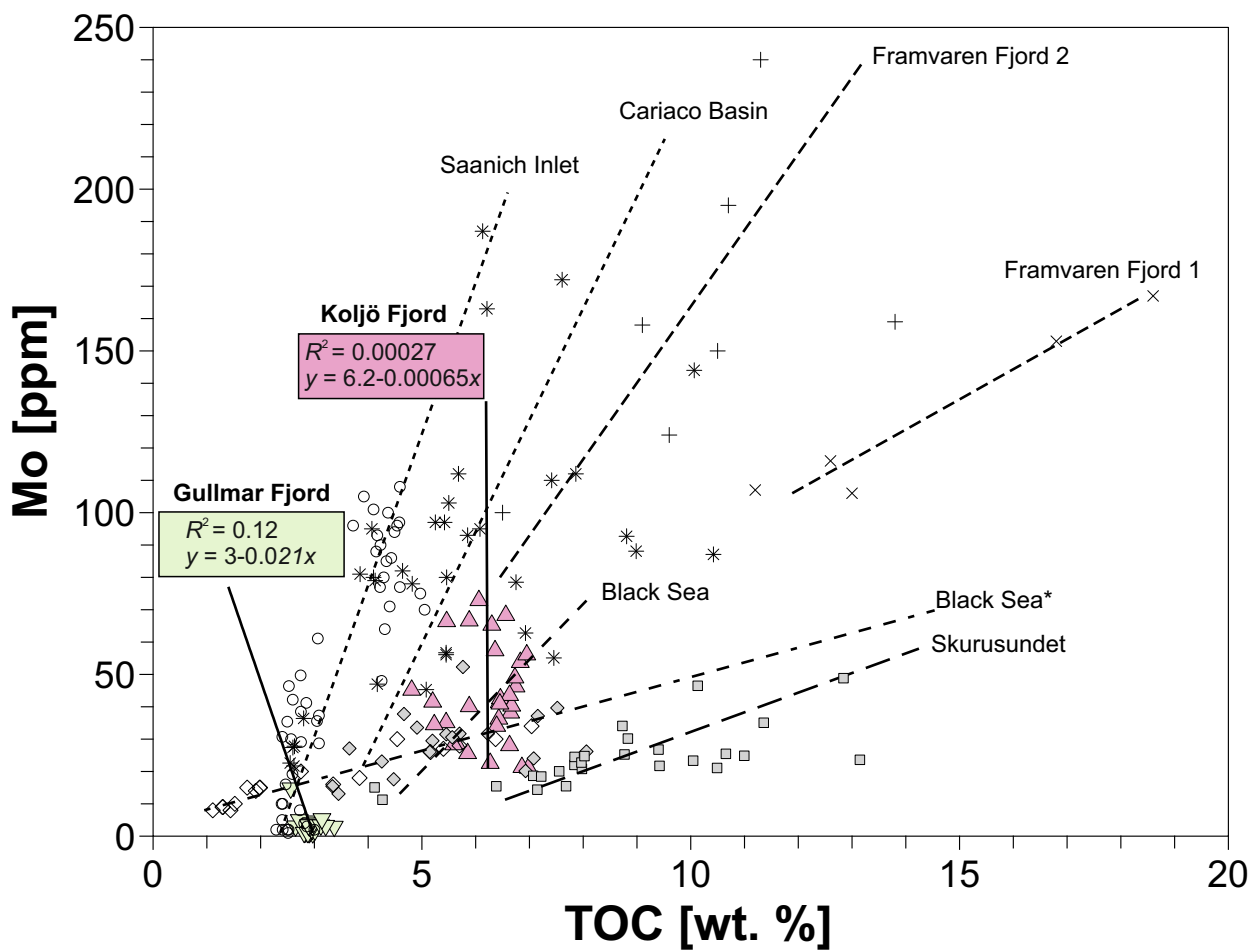
Figure S10. Mo-TOC covariation patterns at Gullmar Fjord (light green-filled reversed triangles) and Koljö Fjord (pink-filled triangles), relative to other coastal marine environments worldwide (unfilled symbols). Grey filled symbols depict data from a parallel study, Skurusundet (St. 7, squares) and Black Sea (PHOXY St. 2, diamonds) (Paul et al., 2023). Regression lines are shown for each site (dashed: literature data, solid: this study). The coefficient of determination (R^2) and slope values are given for the two fjords from this study, for the other sites, see Algeo and Lyons (2006) and Paul et al. (2023). Saanich Inlet data (unfilled circles) comprise three sites: SI-9 (less restricted outer fjord, short gravity core, 38 cm), SN0.8 (restricted inner fjord, short gravity core, 58 cm; both François, 1987), and ODP site 1033 (intermediate fjord, long gravity core 53 m, here only the upper 37 m "Unit I" is considered; Yano et al., 2020). Cariaco Basin data (stars) comprise two sites: PL07-81BC (short core, 15 cm; Calvert et al., 2015), and ODP site 1002 (long gravity cores, 8 and 45 m, here only upper 3.8 and 4.9 m considered; Lyons et al., 2003 and Yano et al., 2020). Framvaren Fjord data are from one site (F1; Skei, 1981, 1988; data retrieved from Algeo and Lyons, 2006), but split into the upper 0–16 cm (1, plus symbols), and lower 16–45cm (2, crosses) sections due to significant changes in Mo-TOC relationships; as per Algeo and Lyons, 2006. Black Sea* (unfilled diamonds) comprise data from three sites: STA 7 (SE slope), STA 9, and STA18A (abyssal plain, box cores ~0–35cm; Algeo and Lyons, 2006).

References

Algeo, T. J. and Lyons, T. W.: Mo -total organic carbon covariation in modern anoxic marine environments: Implications for analysis of paleoredox and paleohydrographic conditions, Paleoceanography, 21, PA1016, https://doi.org/10.1029/2004pa001112, 2006.

Calvert, S. E., Piper, D. Z., Thunell, R. C., and Astor, Y.: Elemental settling and burial fluxes in the Cariaco Basin, Mar. Chem., 177, 607-629, https://doi.org/10.1016/j.marchem.2015.10.001, 2015.

Filipsson, H. L. and Nordberg, K.: A 200-year environmental record of a low-oxygen fjord, Sweden, elucidated by benthic foraminifera, sediment characteristics and hydrographic data, J. Foramin. Res., 34, 277-293, https://doi.org/10.2113/34.4.277, 2004a.

Filipsson, H. L. and Nordberg, K.: Climate variations, an overlooked factor influencing the recent marine environment. An example from Gullmar Fjord, Sweden, illustrated by benthic foraminifera and hydrographic data, Estuaries, 27, 867-881, https://doi.org/10.1007/Bf02912048, 2004b.

François, R.: Some aspects of the geochemistry of sulphur and iodine in marine humic substances and transition metal enrichment in anoxic sediments, PhD dissertation, University of British Columbia, Vancouver, B.C., Canada, 462 pp., https://doi.org/10.14288/1.0053223, 1987.

Jokinen, S. A., Koho, K., Virtasalo, J. J., and Jilbert, T.: Depth and intensity of the sulfate -methane transition zone control sedimentary molybdenum and uranium sequestration in a eutrophic low-salinity setting, Appl. Geochem., 122, 104767, https://doi.org/10.1016/j.apgeochem.2020.104767, 2020.

Kotov, S. and Paelike, H.: QAnalySeries -a cross-platform time series tuning and analysis tool, AGU Fall Meeting Abstracts, PP53D-1230, https://doi.org/10.1002/essoar.10500226.1,

Lyons, T. W., Werne, J. P., Hollander, D. J., and Murray, R. W.: Contrasting sulfur geochemistry and Fe/Al and Mo/Al ratios across the last oxic-to-anoxic transition in the Cariaco Basin, Venezuela, Chem. Geol., 195, 131-157, https://doi.org/10.1016/s0009-2541(02)00392-3, 2003.

Nordberg, K., Gustafsson, M., and Krantz, A. L.: Decreasing oxygen concentrations in the Gullmar Fjord, Sweden, as confirmed by benthic foraminifera, and the possible association with NAO, J. Marine. Syst., 23, 303-316, https://doi.org/10.1016/S0924-7963(99)00067-6, 2000.

Paul, K. M., van Helmond, N. A. G. M., Slomp, C. P., Jokinen, S. A., Virtasalo, J. J., Filipsson, H. L., and Jilbert, T.: Sedimentary molybdenum and uranium: Improving proxies for deoxygenation in coastal depositional environments, Chem. Geol., 615, 121203, https://doi.org/10.1016/j.chemgeo.2022.121203, 2023.

Scholz, F., McManus, J., and Sommer, S.: The manganese and iron shuttle in a modern euxinic basin and implications for molybdenum cycling at euxinic ocean margins, Chem. Geol., 355, 56-68, https://doi.org/10.1016/j.chemgeo.2013.07.006, 2013.

Skei, J.: Et biogeokjemisk studium av en permanent anoksisk fjord–Framvaren ved Farsund (in Norwegian) in: NOVA Rep. F-80400. Nor. Inst. for Vannforsk (NIVA), 108, ISBN 82-577-0447-4, 1981.

Skei, J. M., Loring, D. H., and Rantala, R. T. T.: Partitioning and Enrichment of Trace-Metals in a Sediment Core from Framvaren, South-Norway, Mar. Chem., 23, 269-281, https://doi.org/10.1016/0304-4203(88)90098-9, 1988.

SMHI (Swedish Meteorological and Hydrological Institute): Svenskt HavsARKivs (SHARK) database: Water chemistry data 1950–2018: https://sharkweb.smhi.se/hamta-data/, last access: 03 September 2022.

Yano, M., Yasukawa, K., Nakamura, K., Ikehara, M., and Kato, Y.: Geochemical Features of Redox -Sensitive Trace Metals in Sediments under Oxygen-Depleted Marine Environments, Minerals, 10, 1021, https://doi.org/10.3390/min10111021, 2020.